Highly thermally resistant, hydrophobic poly(vinyl alcohol)–silica hybrid nanofibers

MUSTAFA HULUSI UGUR, BURCU OKTAY, ATILLA GUNGOR
and NILHAN KAYAMAN-APOHAN*

Marmara University, Faculty of Arts and Sciences, Department of Chemistry, 34722, Istanbul, Turkey

Abstract: In this paper, the preparation of hydrophobic and crosslinked poly-(vinyl alcohol)/silica organic–inorganic hybrid nanofibers *via* the sol–gel electrospinning method is reported. Silica was produced through the acetic acid catalyzed reaction of a silica precursor consisting of dimethyldimethoxysilane (DMDMOS), methyltrimethoxysilane (MTMS), tridecafluoro-1,1,2,2-tetrahydrooctyltriethoxysilane (FAS1313; Dynasylan® F 8261) and phenyltrimethoxysilane (PTMS; Dynasylan® 9165) in a 2-propanol–water mixture. Hybrid nanofibers were obtained by electrospinning the silica precursor and an aqueous PVA solution. Chemical, structural, thermal and surface analyses were conducted by Fourier-transform infrared spectroscopy, thermogravimetric analysis, scanning electron microscopy/energy-dispersive X-ray (SEM/EDX) and water contact angle (WCA) methods, respectively. The obtained hybrid nanofibers were insoluble in aqueous solution. SEM images displayed that highly crosslinked and porous structures were obtained and the average fiber diameters of poly(vinyl alcohol) (PVA)/silica nanocomposites were around 70 nm. A nanofiber surface with a water contact angle of 130° was achieved.

Keywords: poly(vinyl alcohol); electrospinning; sol–gel; hybrid nanofibers.

INTRODUCTION

Electrospinning has become a recognized method within the last decade and it is primarily concerned with the preparation of electrospun materials from synthetic and natural polymers. The electrospun materials show different architectures in the large diameter range.[1,2] Electrospinning equipment comprises a pump, a collector and a high voltage supply, which generates between 1–40 kV voltage that orients the polymer solution to the collector. In the electrospinning process, a high voltage is applied to surface of a polymer solution. As the charged solution overcomes its surface tension, a jet travels towards a collector.[3,4]

However, nanofibers are often preferred due to their large surface area to volume ratio.[5] Moreover they show high porosity with a controllable pore structure and tailorable thickness.[6] Nanofibers have huge potential for application in tissue scaffolds, drug release, protective clothing, sensors and affinity membranes.[7] In particular, nanofiber matrices are highly desirable for fabricating scaffolds in tissue engineering because of their porous structure, high elastic modulus and cell-surface interactions.[8,9] Teng *et al*. prepared a novel cyclodextrin-functionalized PVA/SiO$_2$ fibrous membrane by electrospinning with a combined sol–gel method. The adsorption capacity of the membranes was tested for indigo carmine dye.[10] In another study, Wang and Sieh used electrospinning for the preparation of lipase immobilized on poly(vinyl alcohol) nanofibrous membranes. The activity of the immobilized lipase biocomponent of the fibers was tested and their stability over time exposed to humidity and temperatures was evaluated.[11] Guo *et al*. used electrospinning, calcination and surface modification techniques for preparation of composite nanofibrous mats. The surface properties of the amphiphilic electrospun nanofibrous PVA mats was changed to amphiphobic by the grafting of fluoroalkyl silane. The fluorinated mat displayed a higher water contact angle (WCA).[12] In another study, fluoroalkyl silane modified super-hydrophobic electrospun membranes were fabricated. Cellulose acetate nanofibers were prepared by electrospinning, TiO$_2$ nanoparticles were deposited on the cellulose acetate nanofibrous membranes and finally, the surface of the mats was modified by fluoroalkyl silane.[13] Electrospinning usually achieves polycrystalline fibers, which may lower the mobility of charge carriers in devices. This technique has some advantages over *e.g.*, wet chemical methods, such as lower cost, less hazard, higher reproducibility and easier controllability.[15]

In this study, the primary goal was to prepare and develop porous and highly thermally resistant hydrophobic PVA/silica hybrid nanofiber mats. The cross-linked PVA/silica nanofibers were synthesized *via* the sol–gel electrospinning technique. The effect of the sol–gel concentration on the morphology, thermal resistance, FTIR spectrum, contact angle and physical properties of the mats were investigated.

EXPERIMENTAL

Apparatus and reagents

Methyltrimethoxysilane (MTMS; Dynasylan® MTMS), phenyltrimethoxysilane (PTMS; Dynasylan® 9165) and tridecafluoro-1,1,2,2-tetrahydrooctyltriethoxysilane (FAS1313; Dynasylan® F 8261) were kindly supplied by EVONIK. Dimethyldimethoxysilane (DMDMOS), poly(vinyl alcohol) (PVA; $\overline{M}_w$ 67,000 g mol^{-1}; 86.7–88.7 mol. % hydrolysis) and 2-propanol (2-PA; (CH$_3$)$_2$CHOH) were purchased from Sigma–Aldrich. Deionized water of 18.2 MΩ cm resistivity (Millipore, Anamed–Turkey) was used. All chemicals were used as received without further purification.

Preparation of PVA/silica electrospinning solution

First, a PVA solution (7 wt. %) was prepared in deionized water. The PVA granules were stirred in deionized water for 30 min at room temperature (RT) and then, the temperature of the mixture was raised to 60 °C and constantly stirred for 3 h to obtain a clear solution. This solution was kept in a refrigerator overnight.

The silica precursor was prepared using MTMS (11.76 g, 0.0864 mol), DMDMOS (5.04 g, 0.042 mol), PTMS (0.72 g, 0.00363mol) and FAS1313 (1.2 g, 0.00234 mol). The mixture of the alkoxysilanes was magnetically stirred for about 1 h at RT. Then, the MTMS/DMDMOS/ /PTMS/FAS1313 mixture were dissolved in 2-propanol (35 mL) and deionized water (65 mL). The mole ratio of the ingredients was 37:160:1000 alkoxysilanes:2-propanol:water. The silica precursor (0.5 to 40 wt. %) was added to the PVA solutions and stirred at 60 °C for 2 h to homogenize the PVA/MTMS/DMDMOS/PTMS/FAS1313 (Table I). Upon adding acetic acid as a catalyst into the prepared solutions, the solutions were immediately electrospun.

TABLE I. Amounts of silica precursor in the aqueous PVA solutions

Nanofiber formulation	Silica precursor wt. %	7 wt.% aq. PVA mL	Nanofiber diameter nm
M1	0.5	99.5	45–75
M2	1	99	48–60
M3	5	95	25–52
M4	10	90	50–100
M5	20	80	15–40
M6	30	70	20–60
M7	40	60	25–100

In total, seven electrospun solutions were prepared containing various amounts of silica precursor. These clear solutions were loaded into a 10 mL stainless steel syringe. The distance between the aluminum foil coated collecting drum and the capillary was fixed as 16 cm. An electric field of 33 kV was applied to the spin solution and the flow rate was kept at 1 mL h^{-1}. Then, the nanofibers were cured at 100 °C for 1 h to obtain the crosslinked materials. A schematic illustration of the resulting PVA/silica nanofibers is shown in Fig. 1.

Characterization

The FTIR spectra of PVA/silica nanofibers were recorded in range of 4000–600 cm^{-1}, using a PerkinElmer Spectrum 100 ATR-FTIR spectrophotometer.

The thermal stability of the samples was tested in the temperature range of 30–600 °C on a Pyris 1 TGA model using a PerkinElmer STA 6000 instrument under a nitrogen flux at a heating rate of 10 °C min^{-1}.

The synthesized pure electrospun PVA/silica nanofibers were characterized by SEM imaging using on a Philips XL30 ESEM-FEG/EDAX microscope. The specimens were prepared for SEM by freeze fracturing in liquid nitrogen and application of a gold coating.

The wettability characteristics of nanofiber coatings were examined on a Kruss (Easy Drop DSA-2) tensiometer. The contact angles (θ) were measured by means of the sessile drop test method in which drops were created using a syringe. Measurements were made using 3–5 μL drops of distilled water. For each sample, at least five measurements were made, and the average was taken. The surface energy of the coatings was calculated. For the calculation of

the surface energy, three test liquids were considered: water and ethylene glycol as polar solvents and diiodomethane as a disperse solvent.
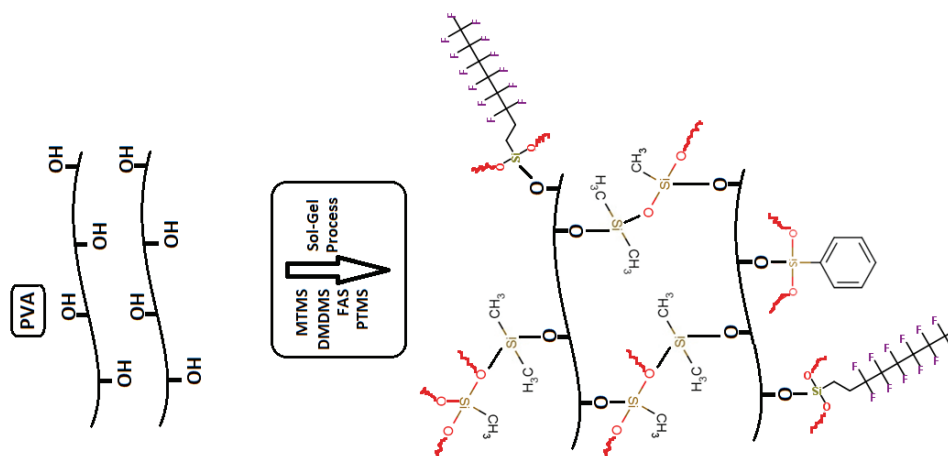

Fig. 1. Schematic illustration of PVA/silica nanofiber mats.

RESULTS AND DISCUSSION

The FTIR spectra of the electrospun PVA-based nanofibers were collected (Fig. 2). As can be seen in Fig. 2, in the spectrum of neat PVA, a large broad band of hydroxyl (OH) stretching appeared at 3300 cm^{-1}. A band at 2850–2950 cm^{-1}, related to CH$_2$ stretching, was also observed. The peak at 1100 cm^{-1} indicated the terminal polyvinyl groups.[16–19] The bands at the 1335 and 1418 cm^{-1} were related to CH bending and CH$_2$ deformation vibrations, respectively[20] and a C–O stretching band was present at 1150–1250 cm^{-1}.

In the FTIR spectra of M1 and M3, Si–O–C and Si–O–Si asymmetric stretchings were observed at 956 and 1135 cm^{-1}, respectively, and they display a broad absorption due to hydrogen-bonded silanols. The Si–O–Si group arises from the reaction between Si–OH and the Si–O–C groups. In this study, the Si–O–Si groups occurred from the reaction between Si–OH groups of hydrolyzed MTMS–DMDMOS–PTMS–FAS1313 and the hydroxyl groups of PVA. The presence of the peaks at 956 and 1135 cm^{-1} demonstrated covalent linkage of PVA and MTMS–DMDMOS–PTMS–FAS13. The FT-IR results proved that a cross--linked network was formed between the organic and inorganic components.[19,21] The absorption at 1725 cm^{-1} arises from C=O stretching in the partially hydrolyzed PVA.[22]

In comparison of the FTIR spectrum of neat PVA, the absorption peak at 3300 cm^{-1} of O–H was absent in the spectra of PVA/silica, which could be attributed to the lack of uncondensed Si–OH and/or unreacted –OH groups of the PVA. Thus, the relative decrease in the intensity of the –OH stretching at 3300

cm^{-1} for PVA/silica-based nanofibers is consistent with the decrease in PVA content in the precursor mixture due to cross-linking between the hydroxyl groups of PVA and the silica sol.
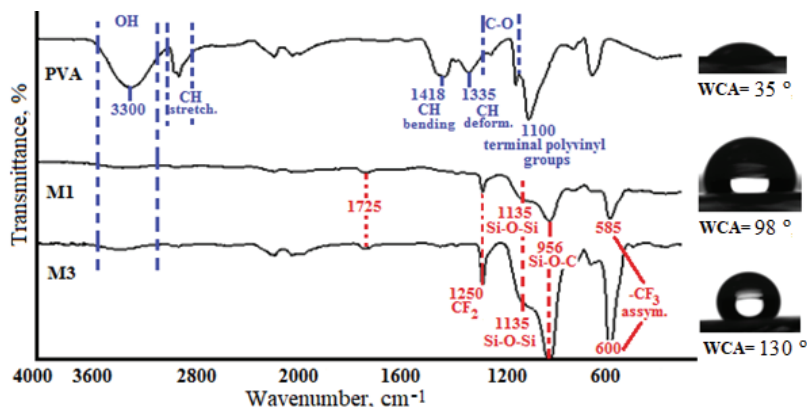

Fig. 2. FTIR spectra of neat PVA and M1 and M3 nanofibers.

The thermal behavior of PVA/silica nanofibers was performed using TGA. The TG and DTG curves of the PVA-based nanofibers containing different contents of the silica precursor are shown in Figs. 3 and 4, respectively. The results for the thermal analysis are presented in Table II, from which it is clear that the decomposition temperature of PVA/silica fiber was much higher than that of the neat PVA fiber.[23] The TG curves show that the first weight lost temperatures inc-
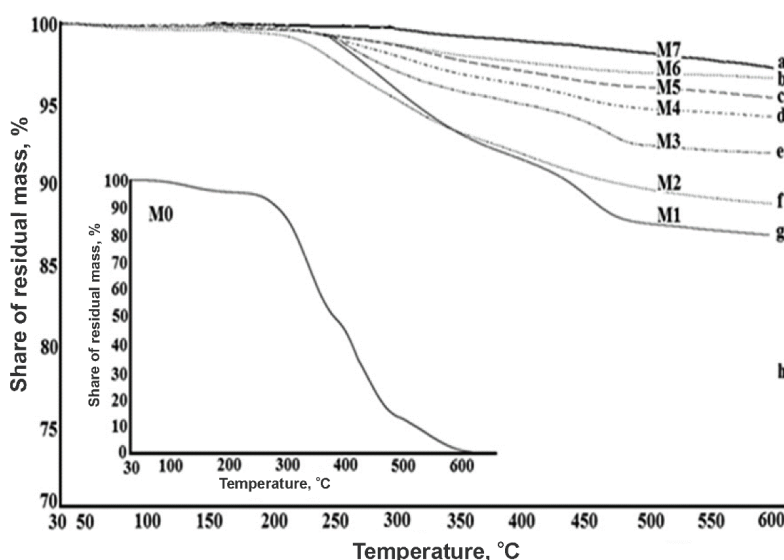

Fig. 3. TGA curves of PVA/silica hybrid nanofibers (a–g) and pure PVA nanofiber (h).

reased with increasing sol–gel ratio for M2 to M7. In addition, the char yield inc-
reased with increasing inorganic content in the nanofibers. It must also be noted
that exceptional char yields were obtained that could be ascribed to the high
thermal stability of the silica precursor used and with the addition of only 0.5 wt.
% silica precursor, the char yield of M1 was calculated as 86 %. The thermal
properties of the resulting PVA/silica nanofibers were better than those obtained
in most other similar studies.[19,23–25] The high thermal stability of the silica pre-
cursor in this work could be attributed to the existence of C–F bonds and rigid
aromatic units. This result also shows that the organic and inorganic matrices
were fully crosslinked at the molecular level as supported previously by the FTIR
results. The enhancement of the rupture energy of the composites due to the high
cross-link density increased the thermal stability of the hybrid nanofiber mats.[23]
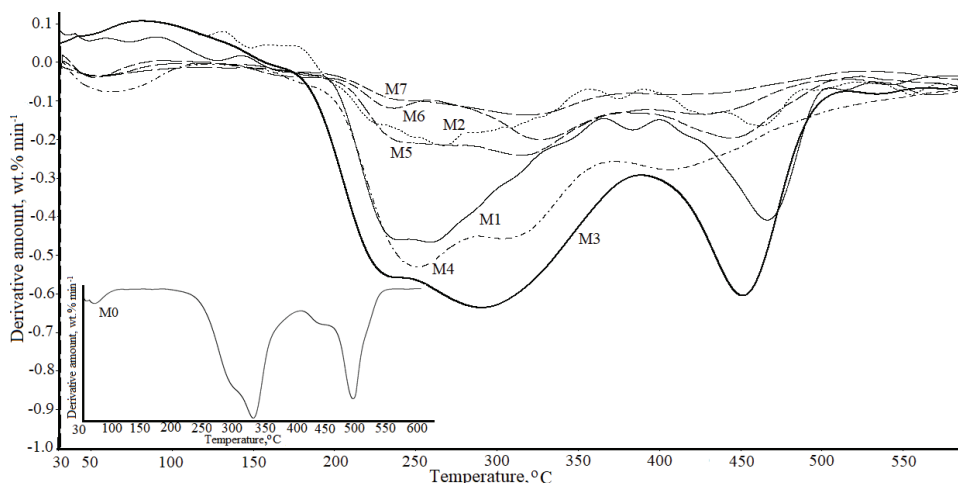

Fig. 4. DTG curves of PVA/silica hybrid nanofibers and pure PVA nanofiber.

TABLE II. Thermal and surface morphology properties of the PVA/silica composite nano-
fibers

Sample code	Silica precursor ratio, wt. %	First weight loss temperature, °C	Char yield %	Water contact angle, °	Surface energy mN m^{-1}
M1	0.5	245	86	98	46.6
M2	1	210	89	110	39.4
M3	5	244	92	130	32
M4	10	255	94	103	43
M5	20	258	95.5	97	51
M6	30	277	97	96	60.8
M7	40	300	98	94	66

The surface properties of the PVA/silica nanofiber mats were examined by
SEM analysis and the water contact angle method. All the micrographs show

different fibrous structures after post-cure at 100 °C for 4 h. The SEM image of pure PVA nanofibers is given in Fig. 5. Figs. 6 and 7 show SEM micrographs of the nanofibers obtained with electrospinning of PVA solutions containing the silica precursor. The SEM images obtained at 40000× and 5000× magnifications are shown in Fig. 6. The average fiber diameters of the obtained hybrid nano-fibers M1 through M4 were found to be 57, 54, 38 and 73 nm, respectively. SEM images displayed evidence that highly cross-linked and beaded nanofibers were obtained. However, more regular, uniform and less beaded samples were formed in comparison of the M5–M7 hybrid membranes.
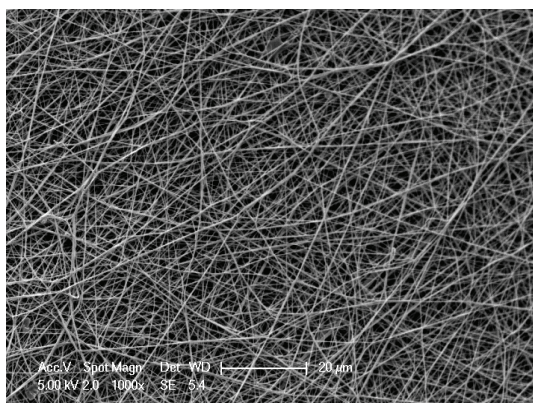

Fig. 5. SEM image of pure PVA nano-fiber.

The elemental distribution on surface of the PVA/silica nanofiber coated aluminum foil (before and after immersion in water) was examined by SEM--EDX analysis (30 kV, 1000×) and the results are given in Table III. The selected region of the micrographs contained mainly C, O and Si coming from PVA/silica hybrid nanofiber. However, Pt came from the coating process before the analysis.

The SEM images of the obtained PVA/silica hybrid nanofibers M5–M7 are presented in Fig. 7, which showed the popcorn-like bead structure of these samples. As shown in Fig. 7 (M5–M7), with increasing the sol–gel ratio from 20 to 40 % (sol volume fraction), the structure resembles an almost fully bead mor-phology.

The SEM micrographs of M3 and M4 after immersion in water (M3-W and M4-W) obtained at magnifications of 40000× and 5000× are shown in Fig. 8. The average fiber diameters the PVA/silica samples M3-W and M4-W were found to be 50 and 59 nm, respectively. When immersed overnight in water, the organic–inorganic nanofibers remained intact, maintaining their morphology, even though PVA has a hydrophilic character. On the other hand, the concentration of inorganic and organic parts are very important and their values should exceed a critical value to maintain a uniform morphology.[26] As can be seen in Fig. 8, both membranes showed very uniform pores.
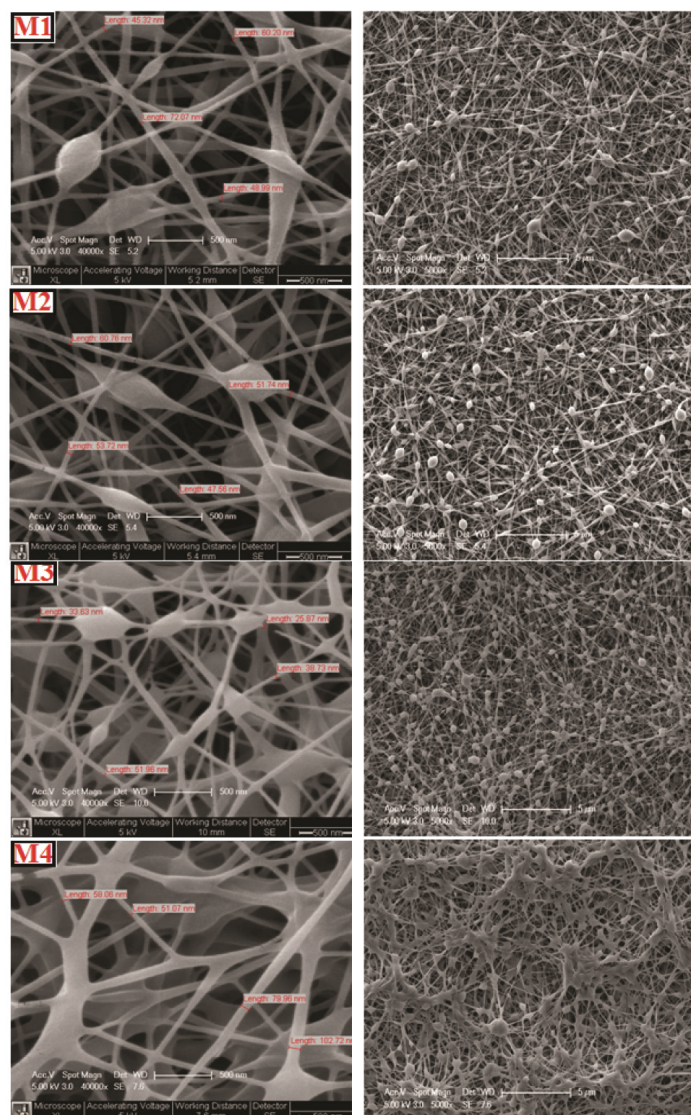
Fig. 6. SEM images of PVA/silica nanofiber mats, M1, M2, M3 and M4, at 40000× and 5000× magnifications (500 nm and 5 µm, from left to right).

Fig. 9 represents an SEM image of a PVA/silica electrospun nanofiber after soaking overnight in water scanned at 1 µm magnification. Fig. 9 (M4-W) shows that pores are widely observed and found to be between 100 and 700 nm. Its SEM image proved that the PVA/silica hybrid membrane (after immersing in water, M4-W) showed very uniform pores. The distribution of pore is very important for filtration, separation and gas permeability applications.
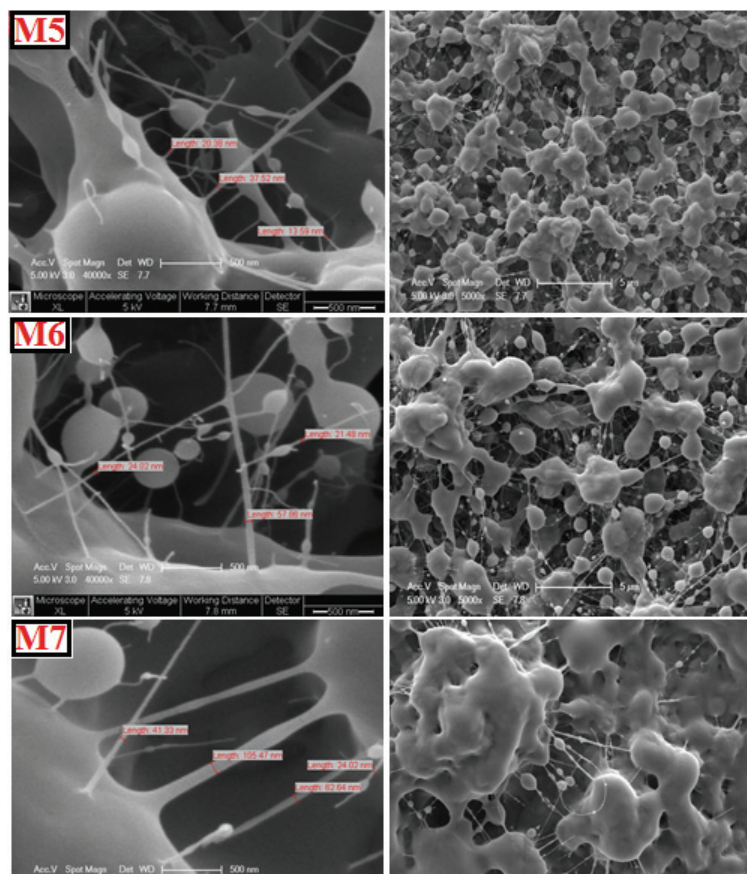
Fig. 7. SEM images of PVA/silica nanofiber mats, M5, M6 and M7, at 40000× and 5000× magnifications (500 nm and 5 μm, from left to right).

TABLE III. EDX results for the PVA/silica composite nanofibers (M1–M4)

Element	Composition before immersion		Composition after immersion	
	wt. %	at. %	wt. %	at. %
M1				
C K	8.72	35.64	8.71	35.89
O K	5.36	16.45	5.15	15.92
Al K	0.2	0.36	0.27	0.49
Si K	17.37	30.35	17.18	30.27
Pt K	68.34	17.19	68.69	17.42
Total	100	100	100	100
M2				
C K	5.31	21.60	5.31	22.17
O K	4.62	14.11	4.77	14.95
Al K	0.58	1.05	0.46	0.85
Si K	27.43	47.70	25.53	45.59

TABLE III. Continued

| Element	Composition before immersion		Composition after immersion	
	wt. %	at. %	wt. %	at. %
		M2		
Pt K	62.05	15.53	63.94	16.44
Total	100	100	100	100
		M3		
C K	5.10	19.78	4.84	19.31
O K	5.07	14.76	4.84	14.50
Al K	0.61	1.06	0.53	0.94
Si K	30.38	50.36	29.58	50.46
Pt K	58.83	14.04	60.21	14.79
Total	100	100	100	100
		M4		
C K	5.46	21.86	4.88	19.73
O K	5.50	16.54	5.27	15.99
Al K	1.30	2.32	1.01	1.82
Si K	25.66	43.97	27.27	47.14
Pt K	62.08	15.31	61.57	15.32
Total	100	100	100	100
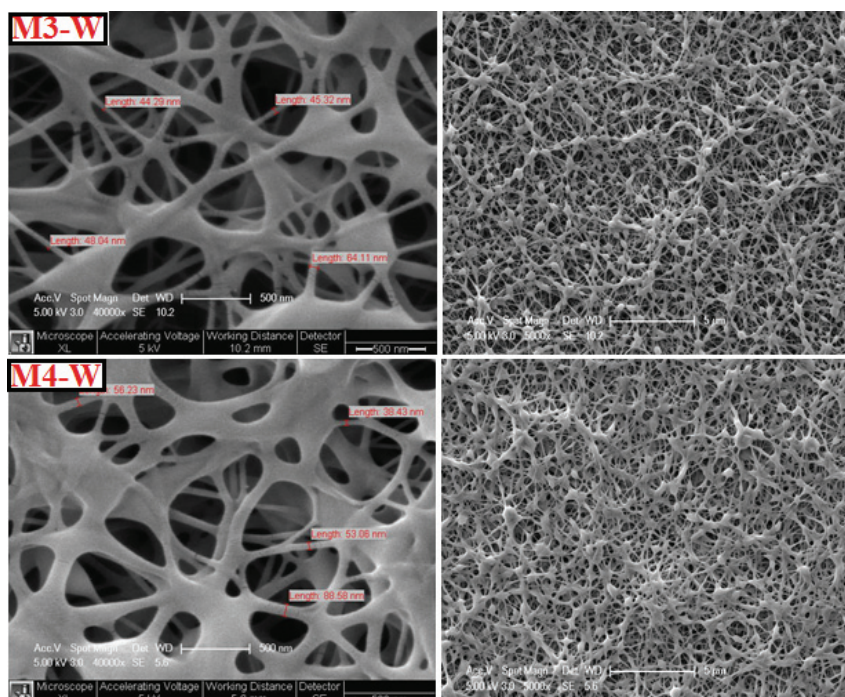
Fig. 8. SEM images of PVA/silica nanofiber mats after being soaked overnight in water, M3-W and M4-W, at 40000× and 5000× magnifications (500 nm and 5 µm, from left to right).
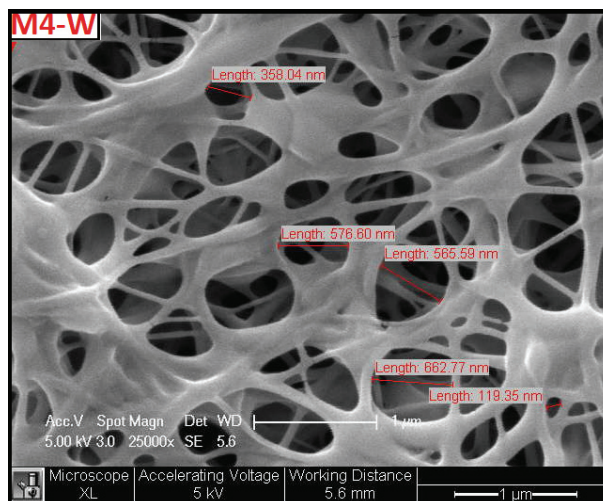
Fig. 9. SEM image of the M4-W PVA/silica nanofiber mat after soaking overnight in water, 25000× magnification (1 µm).

Water contact angles (WCAs) are very sensitive to surface composition changes. The surface properties of PVA and the PVA/silica nanofibers were determined by contact angle measurements. Each given contact angle value represents an average of at least 5 readings. The surface energy and WCA values of the hybrid nanofibers are given in Table II. From the WCA measurements, it was found that with the addition of the silica precursor, the hybrid fibers gained hydrophobic character. While the neat PVA fibers were highly hydrophilic, the hybrid nanofibers displayed contact angle values of around 94–130°. The related WCA images are shown in the FTIR section. There was a slight enhancement in the contact angle as the inorganic content of the coating increased orderly from M1 to M3. The WCA values increased for M1, M2 and M3 by the addition of the inorganic component. The WCA results also showed that the surface energy decreased on addition of the silica precursor due to an increase in its surface roughness. The nanoscale roughness influences the WCA values, in that the WCA value does not depend on compounds of lower surface energy, such as those with $-CH_3$ groups and/or fluoro-containing compounds, but on the hierarchical nanoscale roughness.[27,28] As could be seen in Figs. 6–9, these data suggest that the nanofiber with a reticulate nodes structure markedly contributed to the large WCA.[15] In the present case, while the minimum surface energy was measured to be 32 mN m^{-1}, the corresponding WCA value was 130°, a finding that could be attributed to the low surface energy and highly roughened surface of the hybrid nanofibers. Conversely, the WCA values of the nanofibers began to decrease with the M3 formulation. The increase in the hydrophilicity of the hybrid nanofibers corresponds to an increase in the polarity in the precursor mixture, which

could be attributed to the uncondensed Si–OH and/or unreacted –OH groups of the PVA. Thus, the polar character decreased the surface energy of the hybrid nanofibers going from the M3 to the M7 formulations.

The hydrophobic surfaces have low free surface energies, which is quite advantageous for a variety of properties, such as release and water-repelling properties, biocompatibility, lubricity and durability of materials.[29]

Finally, in comparison with neat PVA nanofibers presented in the literature, the resulting PVA/silica nanofiber mats provide considerable superiority, such as improved thermal resistance, fiber quality and hydrophobicity.[30] The morphologies of neat PVA nanofiber and crosslinked PVA/silica nanofibers were quite different due to the strong interaction between the inorganic and the organic phases. The fact that silica particles were buried in the fibrous structure indicates the compatibility of the phases.

CONCLUSIONS

Cross-linked PVA/silica electrospun mats with reticulated structures with varying percentage of precursor sol, comprising MTMS/DMDMOS/PTMS/ /FAS13, were successfully obtained *via* the electrospinning technique. The cross-linking between PVA chains and the silica network was *via* Si−O−C−O−Si bridges, which was evidenced by the FTIR spectra of the nanofibers. The average fiber diameter was less than 100 nm. SEM images also displayed that the average pore diameter of PVA/silica nanofiber was in range of 100–700 nm. SEM-EDX results showed that when the nanofiber mat was immersed overnight in water, the elemental structure did not change and the fiber remained intact. The 5 wt. % precursor sol containing nanofiber mat had a water contact angle of 130°. The resultant highly thermally resistant hydrophobic PVA/silica hybrid nanofibers with their improved stability in aqueous media could find applications in areas such as filtration, separation, gas permeability and tissue engineering.

И З В О Д

ТЕРМИЧКИ ОТПОРНА И ХИДРОФОБНА ХИБРИДНА НАНОВЛАКНА НА БАЗИ ПОЛИ(ВИНИЛ-АЛКОХОЛА) И СИЛИЦИЈУМ-ДИОКСИДА

MUSTAFA HULUSI UGUR, BURCU OKTAY, ATILLA GUNGOR и NILHAN KAYAMAN-APOHAN

Marmara University, Faculty of Arts and Sciences, Department of Chemistry, 34722, Istanbul, Turkey

У овом раду је приказана израда хидрофобних и умрежених органско–неорганских хибридних нановлакана на бази поли(винил-алкохола)/силицијум-диоксида, поступком сол–гел електроспининга. Силицијум-диоксид је синтетисан реакцијом катализованом присуству сирћетном киселином из прекурсора, који се састојао од диметилдиметокси-силана (DMDMOS), метилтриметоксисилана (MTMS), тридекафлуоро-1,1,2,2-тетрахид-рооктилтриетоксисилана (FAS13; Dinasylan® F 8261) и фенилтриметоксисилана (PTMS; Dinasylan® 9165) у смеши изопропил-алкохола и воде. Хибридна нановлакна су изра-ђена поступком електроспининга полазећи од прекурсора силицијум-диоксида и воде-ног раствора PVA. Хемијски састав и структура, као и термичка и површинска својства

влакана су анализирана помоћу инфрацрвене спектроскопије са Фуријеовим трансфор-мацијама (FTIR), термогравиметријске анализе (TGA), скенирајуће електронске микро-скопије/енергетски дисперзивне рендгенске спектрометрије (SEM/EDX) и контактног угла са водом (WCA), редом. Добијена хибридна нановлакна су нерастворна у воденим растворима. SEM анализа је потврдила густоумрежену и порозну структуру нанокомпо-зитне тканине као и да су вредности пречника нановлакна на бази поли(винил-алко-хола)(PVA)/силицијум-диоксида око 70 nm. Контактни угао са водом на површини нановлакана је износио 130°.

(Примљено 21. новембра 2017, ревидирано 25. јануара, прихваћено 23. фебруара 2018)

REFERENCES

1. S. Agarwal, A. Greiner, J. H. Wendorff, *Prog. Polym. Sci.* **38** (2013) 963
2. B. Oktay, E. Baştürk, N. Kayaman-Apohan, M. V. Kahraman, *Polym. Compos.* **34** (2013) 1321
3. Y. Doshi, D. H. Reneker, *J. Electrost.* **35** (1995) 151
4. K. Garg, G. L. Bowlin, *Biomicrofluidics* **5** (2011) 13403
5. Z. M. Huang, Y. Z. Zhang, M. Kotaki, S. Ramakrishna, *Compos. Sci. Technol.* **63** (2003) 2223
6. C. Feng, K. C. Khulbe, T. Matsuur, S. Tabe, A. F. Ismail, *Sep. Purif. Technol.* **102** (2013) 118
7. K. S. Yang, D. D. Edie, D. Y. Lim, Y. M. Kim, Y. O. Choi, *Carbon* **41** (2003) 2039
8. R. Vasita, D. S. Katti, *Int. J. Nanomed.* **1** (2006) 15
9. S. Y. Lee, D. H. Jang, Y. O. Kang, O. B. Kim, L. Jeong, H. K. Kang, S. J. Lee, C.-H Lee, W. H. Park, B.-M. Min, *Appl. Surf. Sci.* **258** (2012) 6914
10. M. Teng, F. Li, B. Zhang, A. A. Taha, *Colloids Surfaces, A* **385** (2011) 229
11. Y. Wang, Y.-L. Hsieh, *J. Membr. Sci.* **309** (2008) 73
12. M. Guo, B. Ding, X. Li, X. Wang, J. Yu, M. Wang, *J. Phys. Chem., C* **114** (2010) 916
13. T. Ogawa, B. Ding, Y. Sone, S. Shiratori, *Nanotechnology* **18** (2007) 165607
14. M. Gong, X. Xu, Z. Yang, Y. Liu, H. Lv, L. Lv, *Nanotechnol.* **20** (2009) 165602
15. M. G. Gong, Y. Z. Long, X. L. Xu, H. D. Zhang, B. Sun, in *Nanowires – Recent Advances*, X. Peng, Ed., InTech, Rijeka, 2012, Ch. 5, p. 77
16. A. Bandyopadhyay, M. D. Sarkar, A. K. Bhowmick, *J. Mater. Sci.* **41** (2006) 5981
17. A. Hozumi, O. Takai, *Appl. Surf. Sci.* **103** (1996) 431
18. J.-D. Brassard, D. K. Sarkar, J. Perron, *Appl. Sci*. **2** (2012) 453
19. T. Pirzada, S. A. Arvidson, C. D. Saquing, S. S. Shah, S. A. Khan, *Langmuir* **28** (2012) 5834
20. S. Tang, P. Zou, H. Xiong, H. Tang, *Carbohydr. Polym.* **72** (2008) 521
21. R. Guo, X. Ma, C. Hu, Z. Jiang, *Polymer* **48** (2007) 2939
22. J. P. Jeun, Y. K. Jeon, Y. C. Nho, P. H. Kang, *J. Ind. Eng. Chem.* **15** (2009) 430
23. H. Ma, T. Shi, Q. Song, *Fibers* **2** (2014) 275
24. B. Zeytuncu, S. Akman, O. Yucel, M. V. Kahraman, *Mater. Res.* **17** (2014) 565
25. J. M. Dodda, P. Belsky, J. Chmelar, T. Remis, K. Smolna, M. Tomas, L. Kullova, J. Kadlec, *J. Mater. Sci.* **19** (2015)
26. K.-L. Ou, C.-S. Chen, L.-H. Lin, J.-C. Lu, Y.-C. Shu, W.-C. Tseng, J.-C. Yang, S.-Y. Lee, C.-C. Chen, *Eur. Polym. J.* **47** (2011) 882
27. M. Ma, R. M. Hill, *Curr. Opin. Colloid Interface Sci.* **11** (2006) 193
28. Y. Mülazim, E. Çakmakçı, M. V. Kahraman, *J. Vinyl Addit. Technol.* **19** (2013) 31
29. T. Nishino, M. Meguro, K. Nakamae, M. Matsushita, Y. Ueda, *Langmuir* **15** (1999) 4321
30. Z. Peng, L. X. Kong, S. D. Li, *Polymer* **46** (2005) 1949.